International Journal of Mechanics and Energy (IJME)
Vol. 4, Issue 1,2016, ISSN: 2286-5845

Air humidification by forced convection and gas radiation in a cylindrical annular duct

Abir Sakly[1*], Akram Mazgar[1,2], Faycal Ben Nejma[1]

[1]*Preparatory Institute of Engineering Studies of Monastir (IPEIM), Ionized and Reactive Media Studies Research Unit (EMIR), Avenue Ibn Eljazar Monastir 5019, TUNISIA*

[2]*Institute of Applied Sciences and Technology (ISSAT), Mahdia, University of Monastir, Sidi Messaoud, 5111, Mahdia, TUNISIA*

Abstract:

A numerical study is described for combined forced convection and radiative heat transfer. The humid air supposed to be a perfect gas in a boundary layer approached laminar flow is confined between two coaxial cylinders. The inner cylinder, covered by a thin water film, is assumed to be adiabatic, while the outer is thermally insulated and dry. The numerical model, based on the finite volume technique is used to solve the one dimensional Navier-Stokes and energy equations. The radiative part of this study was solved using the "Ray Tracing" method, associated with the "Statistical Narrow Band Correlated–k" (SNBCK) model. This study has been made of the effect of gas radiation and the influence of dry surface emissivity are presented. Results showed that the gas radiation remains non negligible and acts as an influent factor in the humidification process. Also, increasing the dry surface emissivity results in a rising of the humid surface temperature and the evaporated flow rate.

Keywords: Film evaporation, forced convection, thermal radiation, non-grey gas, SNBCK4 model

1. Introduction

Problems involving thermal radiation with combined radiation and forced convection can be encountered in several thermal engineering applications. Heat exchangers, furnace design, thermal insulation, electronic systems, manufacture of papers, and cooling processes in nuclear reactors are some of these thermal engineering application. Generally speaking, heat transfer resulting from coupled processes cannot be separately calculated in such systems. Because of the strong coupling between convection and thermal radiation, some significant errors may occur.

Different kinds of numerical methods are developed in order to solve the radiative transfer equation (RTE). Furthermore, the discrete ordinate method (DOM) as the Ray Tracing method describes variation of radiation intensity as a function of position and angle. The interaction of thermal radiation and free or mixed convection heat transfer is examined by several researchers. The interested readers are referring to [1-5] for detailed reviews. Debbissi et al. [6] analyze water evaporation in a vertical channel including the effects of wall radiation during water evaporation in a vertical channel heated symmetrically by a uniform heat flux density. Sediki et al. [7] also showed that the interaction between mixed convection and radiation for ascending flows in vertical circular tubes. As for internal flows of mixed convection heat transfer, the

*** Correspondingauthor:**Abir Sakly
E-mail: sakly.abir@gmail.com

interactions between hydrodynamic and thermal development become fairly complicated. Debbissi et al. [8], Orfi, et al. [9] and Belhaj Mohamed et al.[10] focus their attention on numerical analysis of water evaporation in humid air in an externally insulated channel. A numerical study is carried out by Chiu and Yan [11] to develop the radiation effect on the characteristics of mixed convection fluid flow and heat transfer in inclined ducts. Their results indicate that radiation effects have a considerable impact on heat transfer and tend to reduce thermal buoyancy effects. Ben Nejma et al.[12] and Mazgar et al.[13] investigate a numerical computation of combined gas radiation and forced convection. A laminar flow of a temperature-dependent and non-grey gas in the entrance region of the channel is investigated. Because of its large absorption bands, over-heated water vapor is considered as an emissive and absorbent non grey gas. A special attention is given to entropy generation and its dependence on geometrical and thermodynamic parameters. Combined radiation and natural convection in humid air flowing into a vertical cylinder and between two isothermal vertical plates is conducted by Mazgar et al. [14] and Ben Nejma and Slimi [15]. It exhibit that the existence of water vapor, even in small quantities, improves the heat transfer rate and increases considerably the evacuated flow rate. The influence of the wall's temperature, the duct's dimensions as well as the vapour molar fraction on the mean Nusselt number and flow rate is also examined and discussed. Mazgar et al.'s analysis [16] is distinctive as they evaluate combined gas radiation and mixed convection in participating media and through a vertical cylindrical annulus. They present the impact of boundary conditions and enclosure dimensions on entropy generation.

Several studies have thoroughly dealt with the interaction between heat and mass transfer. However, the evaluation of gas radiation contribution is often aver looked, specially for investigating the thermal radiation effect on air humidification process and evaporation. This has motivated the current study which aims at investigating the humidification process generated by forced convection and thermal radiation in a cylindrical annulus formed by a wet adiabatic wall and an isothermal dry one.

2. Analysis

2.1. Physical model and assumption

This paper deals with a numerical investigation of combined heat and mass transfers by a steady air forced flow within a duct which is formed by two coaxial and cylinders (graphical abstract). The duct's inner surface is assumed to be adiabatic and wet, while the outer one is supposed to be grey, impermeable and maintained at a constant temperature. The inner cylinder, covered by a thin liquid water film, is considered to be a black body, since water absorbs radiation in the infrared.

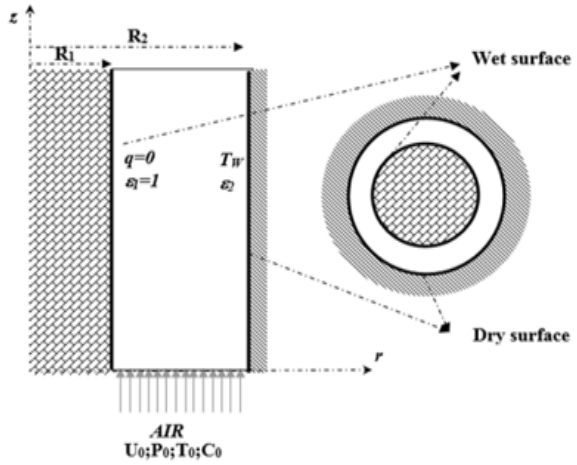

Fig. 1: Physical description of the system

The air flowing across the channel is assumed to be a perfect gas in a boundary layer approached laminar flow. Furthermore, the buoyancy forces, the axial diffusion as well as the Soret and Dufour effects are neglected.The air flowing across the channel is assumed to be a perfect gas in a boundary layer approached laminar flow. Furthermore, the buoyancy

forces, the axial diffusion as well as the Soret and Dufour effects are neglected.

2.2. Model equation

Based on the previous assumptions, the continuity equation and the balances for momentum, mass fraction and energy [6-8] are written as follows:

$$\frac{\partial(\rho r v)}{\partial r}+\frac{\partial(\rho r u)}{\partial z}=0 \quad (1)$$

$$\rho u\frac{\partial u}{\partial z}+\rho v\frac{\partial u}{\partial r}=-\frac{dP}{dx}+\frac{1}{r}\frac{\partial}{\partial r}\left(r\mu\frac{\partial u}{\partial r}\right) \quad (2)$$

$$\rho u\frac{\partial c}{\partial z}+\rho v\frac{\partial c}{\partial r}=\frac{1}{r}\frac{\partial}{\partial r}\left(r\rho D\frac{\partial c}{\partial r}\right) \quad (3)$$

$$\rho C_p u\frac{\partial T}{\partial z}+\rho C_p v\frac{\partial T}{\partial r}=\frac{1}{r}\frac{\partial}{\partial r}\left(r\lambda\frac{\partial T}{\partial r}\right) - div\left(\vec{q}_r\right)+\frac{1}{r}\frac{\partial}{\partial r}\left(r\left(C_{p_v}-C_{p_a}\right)\rho DT\frac{\partial c}{\partial r}\right) \quad (4)$$

The relevant boundary conditions associated with the problem under consideration can be summarized as follows:

Inlet conditions:

$$\begin{cases} v(z=0,\mathrm{r})=0 \\ u(z=0,\mathrm{r})=U_0 \end{cases} \quad (5)$$

$$\begin{cases} c(z=0,\mathrm{r})=C_0 \\ T(z=0,\mathrm{r})=T_0 \end{cases} \quad (6)$$

Wet surface conditions:

$$\begin{cases} \mathrm{v}(z,\mathrm{r}=\mathrm{R}_1)=\dfrac{-D}{1-c(z,r=\mathrm{R}_1)}\dfrac{\partial c}{\partial r}\Big|_{\mathrm{r}=\mathrm{R}_1} \\ u(z,\mathrm{r}=\mathrm{R}_1)=0 \\ \mathrm{c}(z,\mathrm{r}=\mathrm{R}_1)=\dfrac{M_v/M_a}{P/P_{vs}+M_v/M_a-1} \\ -\lambda\dfrac{\partial T}{\partial r}\Big|_{\mathrm{r}=\mathrm{R}_1}+\rho L_v\mathrm{v}(z,\mathrm{r}=\mathrm{R}_1)+q_r(\mathrm{r}=\mathrm{R}_1)=0 \end{cases} \quad (7)$$

Dry surface conditions:

$$\begin{cases} v(z,\mathrm{r}=\mathrm{R}_2)=0 \\ u(z,\mathrm{r}=\mathrm{R}_2)=0 \\ \dfrac{\partial c}{\partial y}\Big|_{\mathrm{r}=\mathrm{R}_2}=0 \\ T(x,\mathrm{r}=\mathrm{R}_2)=T_W \end{cases} \quad (8)$$

The saturated vapor pressure is given by Valcon [24], according to Eq. (9):

$$\log_{10}(P_{vs})=28.59-8.2\times\log_{10}(T)+2.48.10^{-3}\times T-\frac{3142.32}{T} \quad (9)$$

where the saturated vapor pressure is given in atmosphere and temperature in degree Kelvin.

These equations are added to the mass flow rate conservation equation useful to calculate the pressure gradient:

$$\dot{m}(z)=2\pi\int_{R_1}^{R_2}\rho u(z,r)rdr=\rho_0U_0\pi\left(R_2^2-R_1^2\right)+m(0-z) \quad (10)$$

where the evaporating flow rate is calculated by:

$$m(0-z)=2\pi R_1\int_0^z\rho v(z,r=R_1)dz \quad (11)$$

Humid air is regarded as a perfect thermo-dependent gas. The physical properties are related to temperature as follows [15]:

$$\rho=\frac{P}{R.T}\left[(1-x_{H2O})M_{air}+x_{H2O}M_{vapor}\right] \quad (12)$$

$$k=\frac{x_{H2O}k_{vapor}(T)M_{vapor}^{1/3}+(1-x_{H2O})k_{air}(T)M_{airr}^{1/3}}{x_{H2O}M_{vapor}^{1/3}+(1-x_{H2O})M_{airr}^{1/3}} \quad (13)$$

$$\begin{cases} k_{vapor}(T)=\dfrac{1.3\times10^{-6}(1084.7\times T^{1,5}+11.8\times T^{13/6})}{T+160} \\ k_{air}(T)=\dfrac{2.20143\times10^{-3}\times T^{1,5}}{T+134.31} \end{cases} \quad (14)$$

$$Cp = \frac{x_{H2O} M_{vapor}}{\left[(1-x_{H2O})M_{air} + x_{H2O} M_{vapur}\right]} Cp_{vapor}(T) + \frac{(1-x_{H2O})M_{air}}{\left[(1-x_{H2O})M_{air} + x_{H2O} M_{vapor}\right]} Cp_{air}(T) \quad (15)$$

$$\begin{cases} Cp_{vapor}(T) = 1687 + 0.533889T \\ Cp_{air}(T) = 968.76 + 0.067783T \end{cases} \quad (16)$$

$$\mu = \frac{1}{\frac{x_{H2O}}{\mu_{vapor}(T)} + \frac{1 - x_{H2O}}{\mu_{air}(T)}} \quad (17)$$

$$\begin{cases} \mu_{vapor}(T) = \dfrac{3.01472 \times 10^{-5} \times \sqrt{\dfrac{T}{273.15}}}{1 + \dfrac{673}{T}} \\ \mu_{air}(T) = \dfrac{2.53928 \times 10^{-5} \times \sqrt{\dfrac{T}{273.15}}}{1 + \dfrac{122}{T}} \end{cases} \quad (18)$$

$$D(T) = \frac{2.26}{1.013.10^5} \cdot \left(\frac{T}{273.15}\right)^{1.81} \quad (19)$$

$$L_V(T) = 4185.\left(597 - 0,56.(T - 273.15)\right) \quad (20)$$

2.3. Numerical method

The application of the ″statistical narrow band correlated-k (SNBCK) ″ model by Goutière et al.[18] to non-grey gas radiation transfer demonstrate that this model is an efficient narrow-band one for radiative transfer calculation as well as for low-resolution spectral intensity prediction. Using the 4-point Gauss-Legendre quadrature [19], where gas radiative properties are represented by four grey gases at each non-overlapping band, the SNBCK model [20-21] can overcome the difficulties of the SNB model by extracting the gas absorption coefficients from the gas transmissivity given by Malkmus [22]:

$$\bar{\tau}_\nu(L) = \exp\left[-\frac{\pi B}{2}\left(\sqrt{1 + \frac{4AL}{\pi B}} - 1\right)\right] \quad (21)$$

The analytical expression (Eq. 23) of the cumulative function has been derived by Lacis and Oinas [23]:

$$g(\kappa) = \frac{1}{2}\left[1 - erf\left(\frac{a}{\sqrt{\kappa}} - b\sqrt{\kappa}\right)\right] + \frac{1}{2}\left[1 - erf\left(\frac{a}{\sqrt{\kappa}} + b\sqrt{\kappa}\right)\right]\exp^{\pi B} \quad (22)$$

Where $a = \frac{1}{2}\sqrt{\pi AB}$, $b = \frac{1}{2}\sqrt{\frac{\pi B}{A}}$ and *erf* is the error function.

Using the cumulative function *g*, the narrow-band average of any radiative variable ϕ_ν can be calculated as:

$$\bar{\phi_\nu} = \sum_{i=1}^{4} w^i \phi\left(g^i\right) \quad (23)$$

The calculation of the various monochromatic absorption coefficients is thus reduced to the resolution of the system:

$$g(\kappa_\nu^i) = g^i \quad (24)$$

The different absorption coefficient are generated for, three temperatures (400K, 450K, 500K) and twenty water vapor mole fraction (0.05, 0.1,…, 1). The interpolation for intermediate temperatures is forced since the SNB model parameters are available only for certain temperatures. Using the SNBCK4 model allows us to resolve the radiative transfer equation Eq. (25).

The radiative intensity is calculated through the Ray Tracing method, based on the selection of transfer directions and their associated weights. As the finite volume technique is taken into consideration, we chose the 1-D radiative analysis (slab problem), supposing that, the temperature and the mass fraction vary only through radial direction.

$$\frac{dI_\nu^i\left(r,\vec{\Omega}\right)}{dl} = -\kappa_\nu^i I_\nu^i\left(r,\vec{\Omega}\right) + \kappa_\nu^i I_\nu^b \quad (25)$$

Where $I_\nu^i\left(r,\vec{\Omega}\right)$ represents the solution of the following recurrent relation:

$$I_k = \exp\left[-\kappa_\nu^i l_{j_{k+1\to k}}(\vec{\Omega})\right] I_{k+1}\left(r,\vec{\Omega}\right) + \left[1-\exp\left[-\kappa_\nu^i l_{j_{k+1\to k}}(\vec{\Omega})\right]\right] I_\nu^b \tag{26}$$

l is the optical path shown in Fig. 1 and calculated with:

$$l_{j_{k\to k+1}}(\vec{\Omega}) = \left| \frac{\sqrt{\left(1-\eta^2\right) r_{k+1}^2 - r_j^2\xi^2} - \sqrt{\left(1-\eta^2\right) r_k^2 - r_j^2\xi^2}}{1-\eta^2} \right| \tag{27}$$

The scattering effect can be neglected since the medium contains no particles. The surfaces are assumed to be diffusely reflective. The radiative boundary conditions are given as:

$$\begin{cases} I_\nu^i\left(r=R_1,\vec{\Omega}\right) = I_\nu^b\left(T\left(r=R_1\right)\right) \\ I_\nu^i\left(r=R_2,\vec{\Omega}\right) = \dfrac{1-\varepsilon_2}{\pi} \displaystyle\int_{\vec{\Omega}'/\vec{\Omega}'.\vec{n}>0} I_\nu^i\left(r=R_2,\vec{\Omega}'\right)\xi\left(\vec{\Omega}'\right) d\Omega' + \varepsilon_2 I_\nu^b\left(T_W\right) \end{cases} \tag{28}$$

The expression of the radiative flux is given as follows:

$$q_r = \sum_{bands} \int_{4\pi} \sum_{i=1}^{4} \mathrm{w}^i I_\nu^i(\vec{\Omega})\xi(\Omega)\, d\Omega\, \Delta\nu \tag{29}$$

The radiative source term given by Liu et al. [19] is formulated in Eq. (30):

$$div(\vec{q}_r) = \sum_{bands} \int_{4\pi} \sum_{i=1}^{4} \mathrm{w}^i \kappa_\nu^i \left[I_\nu{}^b - I_\nu^i(\vec{\Omega})\right] d\Omega\, \Delta\nu \tag{30}$$

We define the local radiative Nusselt number as follow:

$$Nu_r(z) = \frac{2\left(R_2 - R_1\right)}{R_2} \frac{\displaystyle\int_{R_1}^{R_2} div\left[\vec{q}_r(z,r)\right] r dr}{\left[T_W - T_B(z)\right] k(T_W)} \tag{31}$$

For mass transfer, the local Sherwood number is defined as:

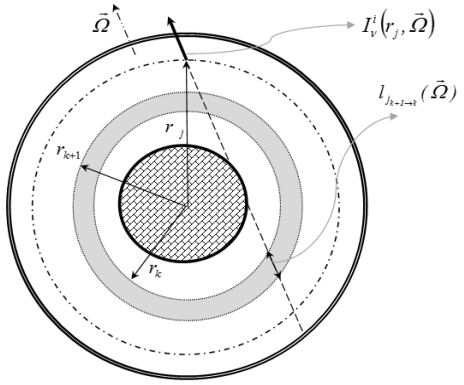

Fig. 2 Optical path

Where the bulk temperature is given by Eq. (32):

$$T_B(z) = \frac{\displaystyle\int_{R_1}^{R_2} \rho(r,z) C_P(r,z) u(r,z) T(r,z) r dr}{\displaystyle\int_{R_1}^{R_2} \rho(r,z) C_P(r,z) u(r,z) r dr} \tag{32}$$

The finite volume method is applied to solve numerically the set of governing conservation Eq. (1-4). A uniform 50-nodes grid according to the radial direction and a Tchebychev's sinusoidal 300-nodes grid according to the axial direction are used. The utilization of a sinusoidal grid helped enormouslyto ensure theconvergenceof the iterative process.

$$\Delta z_i = L_z\left[\cos\left(\frac{\pi}{2}\frac{i-1}{N_z}\right) - \cos\left(\frac{\pi}{2}\frac{i}{N_z}\right)\right] \tag{33}$$
$$1 \le i \le N_z$$

$$\Delta r = \frac{R_2 - R_1}{N_r} \tag{34}$$

This grid is chosen as a tradeoff between the computational time and the accuracy as shown in Table 1. The present numerical study is checked for accuracy against numerical results published earlier and reported by Liu et al. [19]. The numerical predictions of heat flux density at the wall are also compared to those given by Liu et al., where water vapor kept at 1atm and 1000K is introduced between

two black plates maintained at 0K and separated by a thickness e.

Table 1 Effect of the grid size on the evaporating flow rate R_1=0.1m, R_2=0.15m, U_0=0.1m/s, C_0=0, P_0=1atm, T_0=300K, T_W=500K, $\varepsilon_1=\varepsilon_2$=1, z=2m

Grid (r:z)	50:100	**50:300**	100:300	100:500
$m(0-z)$ (g/s) without radiation	0.02738	**0,02716**	0.02703	0.02698
$m(0-z)$ (g/s) with radiation	1.34493	**1.34528**	1.34605	1.34672

Table 2 Validation of the SNBCK implementation

	Liu et al. [19]		*Present work (SNBCK4)*		
	SNB	*SNBCK4*	***S_4***	*S_6*	*S_8*
e= 0.1m	-14.2	-14.3	**-14.60**	-14.56	-14.40
e = 1m	-30.3	-30.6	**-31.00**	-30.87	-30.81

To be in a geometrical situation comparable to that of Liu et al., we consider the case of an annular enclosure with infinite radii. The results are very close as shown in Table 2 where the S4 quadrature, adopted as the numerical method to solve the radiative coupling problem, can be seen to have reasonable accuracy.

3. Results and discussion

In fig. 2, the variations of temperature, axial velocity and mass fraction are given for different annular sections, in both thermal radiation configurations, with and without gas radiation. We can be noted a rising in the temperature of the internal cylinder. This is visible for both thermal radiation situations and is generating due to radiative exchanges between surfaces. The inner wall temperature is significantly lower compared to the outer one because of the energy consumed to ensure water evaporation. In the first axial zone of the flow, we distinguish the appearance of two fluid behaviors. In fact, in vicinity of the inner wall, where the vapor migration has forced the media to contribute to radiative exchanges, the fluid temperatures are greater when gas radiation is taken into consideration. Close to the dry surface, temperature profiles are confounded in both thermal radiation configurations because of gas transparency. It can also be signaled also that the minimum temperature valuemigrates from the central zone of the flow to be stabilized at the inner surface, a revealing sign of reaching the conductive effect.Examining the mass fraction fields displays profiles with high gradients in the vicinity of the inner surfaceand substantially stable profiles close to the outer wall. These gradients are less pronounced as well as we advance through the duct. Moreover, the fact that the temperature of the inner surface is slightly larger in absence of gas radiation, this conditions the saturated vapor pressure and makes mass fraction at its upper limit, which results in a slightly higher gradients, accentuating the evaporation process.

Dry surface emissivity effect

It is worth noting that the effect of wall emissivity is very significant as it can be shown by the variations of the local radiative Nusselt number through axial position (Fig. 3). In fact, reducing wall emissivity favorites gas-gas exchanges to the detriment of surface-surface and gas-surface exchanges. We distinguish therefore a decrease in the radiative Nusselt number when reducing wall emissivity. As the principal thermal radiation source is the dry cylinder, increasing its wall emissivity will certainly enhance radiative transfers, this results in, a rising of the humid surface temperature, an augmentation in the saturated vapor pressure

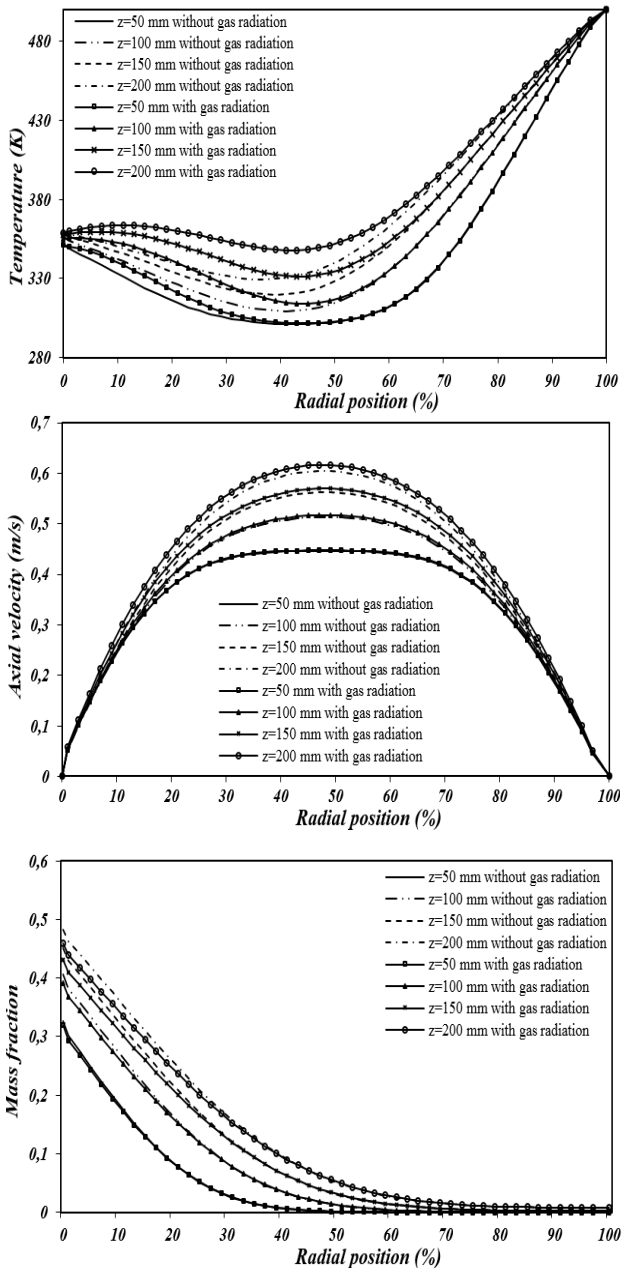

Fig.3 Temperature, axial velocity and mass fraction profiles

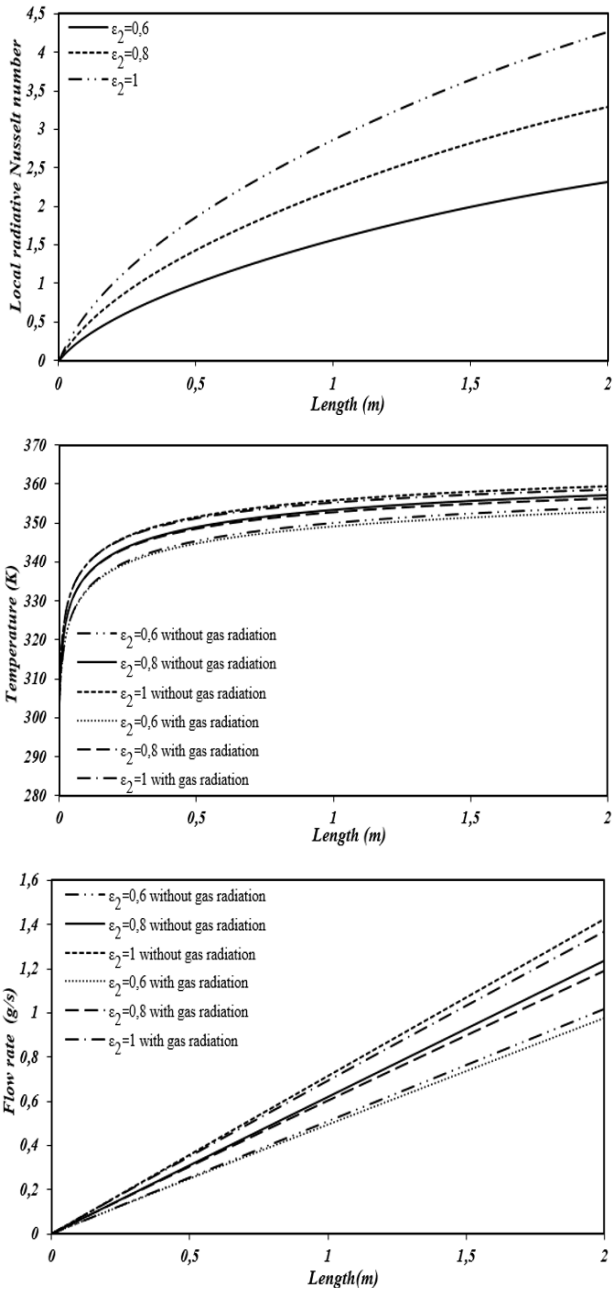

Fig.4 Influence of the emissivity on local radiative Nusselt number, wet cylinder temperature and evaporating flow rate profiles

increasing the mass fraction of water vapor and consequently an enhancement in mass transfer. Furthermore, we can point at each annulus section and for both thermal radiation configurations, the reduction of the difference in the wet temperature, using a regular interval of emissivity difference. Moreover, and for a given annulus section, we notice a uniformity of the difference between the inner wall temperature when gas radiation is not taken into

account and that calculated with gas radiation. The repercussions on mass transfer
are imminent; this is clearly visible in the evaporated mass profiles which seem to have linear evolutions.

4. Conclusion

A numerical study is developed to estimate heat and mass transfer for a steady and not fully developed flow in a duct made up of two-coaxial cylinders: the inner cylinder covered by a thin water film, is assumed to be adiabatic while the outer one is isothermal and dry.

Basedon the results we can conclude that even if it is not the dominant heat transfer mode, gas radiation remains non negligible and acts as an influent factor in the humidification process.The use of a higher dry surface emissivity results in a rising of the humid surface temperature and the evaporated flow rate. Also, the presence of gas radiation reduces nevertheless the wet wall temperature and contributes to its surface protection.

Nomenclature

c mass fraction of water vapor
C_p specific heat ($J.kg^{-1}.K^{-1}$)
C_{pa} specific heat for air ($J.kg^{-1}.K^{-1}$)
C_{pv} specific heat for water vapor ($J.kg^{-1}.K^{-1}$)
D diffusion coefficient (m^2s^{-1})
I radiation intensity ($W.m^{-2}.sr^{-1}$)
k thermal conductivity ($W.m^{-1}.K^{-1}$)
L_v latent heat of evaporation ($J.kg^{-1}$)
m flow rate (g/s)
M_a molar mass of air ($kg.mol^{-1}$)
M_v molar mass of water vapor ($kg.mol^{-1}$)
Nu_r local radiative Nusselt number
P pressure (Pa)
q heat flux ($W.m^{-2}$)
R gas constant ($J.mol^{-1}.K^{-1}$)
R_1 internal radius (m)
R_2 external radius (m)
T temperature (K)
u axial velocity ($m.s^{-1}$)
v radial velocity ($m.s^{-1}$)
w weight parameter
r,z cylindrical coordinates

Greek symbols

ν wave number (cm^{-1})
ε emissivity
κ absorption coefficient (m^{-1})
$\Delta\nu$ spectral resolution ($\Delta\nu = 100 cm^{-1}$)
$d\Omega$ elementary solid angle
λ thermal conductivity ($W.m^{-1}.K^{-1}$)
μ dynamic viscosity ($N.s.m^{-2}$)
ρ density of the fluid ($Kg.m^{-3}$)
χ, ξ, η director cosines

Subscripts

r radiative exchange
0 ambient
ν spectral

Superscripts

b black body
i grey gas associated

References

[1] L.K. Yang, Combined mixed convection and radiation in a vertical pipe, Int. Commun. Heat Mass Transfer 18 (1991) 419-430.

[2] L.K. Yang, Forced convection in a vertical pipe with combined buoyancy and radiation effects, Int. Commun. Heat Mass Transfer 19 (1992) 249-262.

[3] T. Seo, D.A. Kaminski and M.K. Jensen, Combined convection and radiation in simultaneously developing flow and heat transfer with nongray gas mixtures, Numer. Heat Transfer Part A 26 (1994) 49-66.

[4] W.M. Yan, H.Y. Li and D. Lin, Mixed convection heat transfer in a radially rotating square duct with radiation effects, Int. J. Heat Mass Transfer 42 (1999) 35-47.

[5] W.M. Yan and H.Y. Li, Radiation effects on mixed convection heat transfer in a vertical square duct, Int. J. Heat Mass Transfer 44 (2001) 1401-1410.

[6] C. Debbissi, J. Orfi and S. Ben Nasrallah, Evaporation of water by free convection in a vertical channel including effects of wall radiative properties, Int. J. Heat Mass Transfer 44 (2001) 811-826.

[7] E. Sediki, A. Soufiani and M.S. Sifaoui, Combined gas radiation and laminar mixed convection in vertical circular tubes, Int. J. Heat Fluid flow 24 (2003) 736-746.

[8] C. Debbissi, J. Orfi and S. Ben Nasrallah, Evaporation of water by free or mixed convection into humid air and superheated steam, Int. J. Heat and Mass Transfer 46 (2003) 4703-4715.

[9] J. Orfi, C. Debbissi, A. BelHaj Mohamed and S. Ben Nasrallah, Air humidification by free convection in a vertical channel, Desalination168 (2004) 161-168.

[10] A. Belhadj Mohamed, J. Orfi, C. Debissi and S. Ben Nasrallah, Condensation of water vapor in a vertical channel by mixed convection of humid air in the presence of a liquid film flowing down, Desalination 204 (2007) 471-481.

[11] H.C. Chiu and W.M. Yan, Mixed convection heat transfer in inclined rectangular ducts with radiation effects, Int. J. Heat Mass Transfer 51 (2008) 1085-1094.

[12] F. Ben Nejma, A. Mazgar, N. Abdallah and K. Charrada, Entropy generation through combined non-grey gas radiation and forced convection between two parallel plates, Energy 33 (2008) 1169-1178.

[13] A. Mazgar, F. Ben Nejma and K. Charrada, Numerical analysis of coupled radiation and laminar forced convection in the entrance region of a circular duct for non-grey media: entropy generation, WSEAS Transactions on Heat and Mass Transfer 3 (2008) 165-176.

[14] A. Mazgar, F. Ben Nejma and K. Charrada, Entropy generation through combined non-grey gas radiation and natural convection in vertical pipe, Progress in Computational Fluid Dynamics 9 (2009) 495-506.

[15] F. Ben Nejma and K. Slimi, Combined natural convection and radiation in humid air bounded by isothermal vertical walls, High Temp - High Press 39 (2010) 209-226.

[16] A. Mazgar, F. Ben Nejma, K. Charrada, Second law analysis of coupled mixed convection and non-grey gas radiation within a cylindrical annulus, Int. J. of Mathematical Models and Methods in Applied Sciences 7 (2013) 265-276

[17] M. Agunaoun, A. Daif, R. Barriol and M. Daguenet, Evaporation en convection forcée d'un film mince s'écoulant en régime permanent, laminaire et sans onde, sur une surface plane inclinée, Int. J. Heat and Mass Transfer 37 (1994) 2947-2956.

[18] V. Goutière, F. Liu and A. Charrette, An assessment of real-gas modeling in 2D enclosures, J. Quant. Spectrosc. Radiat. Transfer 64 (1999) 299-326.

[19] F. Liu, G.J. Smallwood and Ö.L. Gulder, Application of the statistical narrow-band correlated-k method to low-resolution spectral intensity and radiative heat transfer calculations-effects of the quadrature scheme, Int. J. Heat and Mass Transfer 43 (2000) 3119-3135.

[20] F. Ben Nejma, A. Mazgar and K. Charrada, Volumetric and wall non grey gas entropy creation in a cylindrical enclosure, WSEAS Transactions on Heat and Mass Transfer 5 (2010) 217-226.

[21] F. Ben Nejma, A. Mazgar and K. Charrada, Application of the statistical narrow-band correlated-k model to entropy generation through non-grey gas radiation inside a spherical enclosure, Int. J. of Exergy 8 (2011) 128-147.

[22] W. Malkmus, Random Lorentz band model with exponential-tailed S^{-1} line-intensity distribution function, J. Opt. Soc. Am. 57 (1967) 323-329.

[23] A.A. Lacis and V. Oinas, A description of the correlated k distribution method for modeling non gray gaseous absorption, thermal emission, and multiple scattering in vertically inhomogeneous atmospheres, J. Geophys. Res. 96 (1991) 9027-9063.

[24]Valcon M., Etude de l'évaporation en convection naturelle, P.H.D. thesis, Poitiers university-France (1979).